Al-Nahrain Journal for Engineering Sciences (NJES) Vol.20 No.1, 2017 pp.149 - 157

Evaluation Performance of Iterative Algorithms for 3D Image Reconstruction in Cone Beam Geometry

Noor H. Fallooh Al-anbari
Electronic and Communications Eng. Dep.,
College of Engineering, Al-Nahrain University,
Baghdad, Iraq
anoornhf87@gmail.com

Mohammed H. Ali Al-Hayani
Electronic and Communications Eng. Dep.,
College of Engineering, Al-Nahrain University,
Baghdad, Iraq
malhayani@gmail.com

Abstract

Algebraic reconstruction technique (ART) is iterative reconstruction algorithm using for reconstructing the two dimension (2D) and three dimension (3D) images. In this research different algorithms of ART were used to reconstruction : (simple ART, Simultaneous ART, and Multiplicative ART) for reconstruction 3D image using multi slice scanner in cone beam geometry. To perform the time reconstruction of ART algorithms, use the Maximum-Likelihood Expectation Maximization (ML-EM) algorithm to fast ART algorithm. Multi slice Computed Tomography CT scanner newly discovered and used widely in the medical field for diagnosis and radiographic to its benefit from the speed of scanner and quality of image reconstruction comparing with single slice scanner. In simulation result the Multiplicative ART (MART) algorithm with suitable relaxation parameter λ used that give best result as shown in this work.

Key word: Computed Tomography CT, Algebraic Reconstruction Technique ART, Multi Slice Cone Beam (MSCB), Multiplicative ART.

1- Introduction

Computed Tomography is commonly called "CT". CT is a way of using X-rays to take pictures or images in very fine slices through the part of the body that which need to investigate. When CT scanners were first invented, they took one slice at a time. Most modern scanners now take more than one slice at a time (range from 4 to 64 slices and up to 320 slices). This is referred to as "multi-slice" or "multi-detector" technology. The multi-slice CT scanning using spiral or helical scanners has resulted in a revolution for diagnostic imaging and gives scanning faster; dosage used optimal, reconstruction algorithms more efficient [1]. The cone-beam geometry was developed as an alternative to conventional CT using either fan-beam or spiral-scan geometries, to provide more rapid acquisition of a data set of the entire field of view (FOV) and it uses a comparatively less expensive radiation detector. Obvious advantages of such a system, which provides a shorter examination time, include the reduction of image unsharpness caused by the translation of the patient, reduced image distortion due to internal patient movements, and increased x-ray tube efficiency. However, its main disadvantage, especially with larger FOVs, is a limitation in image quality related to noise and contrast resolution because of the detection of large amounts of scattered radiation [2].

2- Multi Slice Cone Beam Scan

The multi-slice CT scanner refers to a special CT system equipped with a multiple-row detector array to simultaneously collect data at different slice locations [3].The multi-slice CT scanner has the capability of rapidly scanning large longitudinal (z) volume with high z-axis resolution, and also presents new challenges and new characteristics. There are two modes for a CT scan of cone beam (3D): step-and-shoot CT and helical /spiral CT as shown in figure (1). For step-and-shoot CT, it consists of two alternate stages: data acquisition and patient positioning the patient remains stationary and the x-ray tube rotates about the patient to acquire a complete set of projections at a prescribed scanning location [4] To geve scan slices in size of a few millimeters.

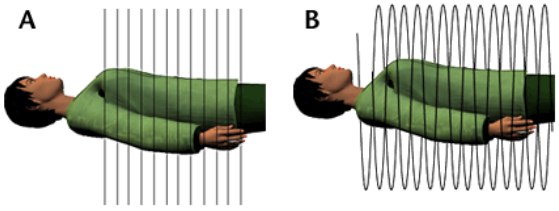

Figuer 1: Conventional CT scans take pictures of slices.

The newer spiral (also called helical) CT scan takes continuous pictures of the body in a rapid spiral motion, so that there are no gaps in the pictures collected. During the data acquisition stage, the patient remains stationary and the x-ray tube rotates around the patient to acquire a complete set of projections at a prescribed scanning location. In the patient positioning stage, no data are acquired and the patient is transported to the next prescribed scanning location. The data acquisition stage typically takes one second or less while the patient positioning stage is around

one second. Thus, the duty cycle of the step-and-shoot CT is 50% at best. This poor scanning efficiency directly limits the volume coverage speed versus performance and therefore the scan throughput of the step-and-shoot CT. The volume coverage speed performance, the capability of rapidly scanning a large longitudinal (z) volume with high longitudinal (*z*-axis) resolution and low image artifacts, is a deciding factor for the success of many medical CT applications which require a large volume scanning (lung) with high image quality and low image artifacts and short time duration. Thus, one of the main themes in CT development is to improve its volume coverage speed performance. The data are continuously collected without pausing, therefore the duty cycle of the helical scan is improved to nearly 100% and the volume coverage speed performance can be substantially improved [4].

3- Reconstruction Algorithms

There are many algorithms used in the reconstruction image from projections, the two major categories of algorithms are; analytical and iterative algorithms. Analytical that is founded on the Fourier Slice Theorem. Many iterative algorithms are available to solve the system of linear equations or to minimize an objective function, involve ART. In this research dealt with the study and implementation of algebraic methods to reconstruction the tomographic [5, 6].

4- Iterative Methods

There are large varieties of ART algorithms, each starting from an initial guess for the reconstruction of the body and then lead a series of estimates grid projections and correct backprojections until converged reconstruction [5]. It is assumed the cross-sections consist of arrays of unknowns and reconstruction problem can be formulated as a system of linear equations are the next steps choosing a finite collection of basic functions and a method to solve the systems [7]. Algebraic techniques are use to produce results with the accuracy desired in medical imaging also useful when the energy propagation paths between the source and receiver positions are subject to ray bending on account of refraction, or when the energy propagation undergoes attenuation along ray paths as in emission CT[8]. In the perception of algebraic for tomographic imaginable assume that the body reconstructing (in cross section 2D CT or size in 3D) contain an unknown matrix, and then algebraic equations solved for the matrix in terms of data examined estimation.

The issue of this work to rebuild a three-dimensional, so it will be assumed that the volume of reconstructing set contains voxels *f(x,y,z)* which are placed in cubic grid. In each cell the function *f(x,y,z)* is constant. Let f_j denote the constant value in the j^{th} cell and let N be the total number of cells. A ray is a line running through the *(x,y,z)*-volume. The projections will be represented as three dimensional matrix, the $p_{kl\theta}$ is the ray sum placed in k^{th} row and l^{th} column of the 2D projection with angle θ, the relationship between the f_j (intensity of each pixel) and $p_{kl\theta}$ represented as :

$$p_{kl\theta} = \sum_{j=1}^{N} w_{jkl\theta} \cdot f_j \quad \dots (1)$$

Where $w_{jkl\theta}$ is a weighting factor that represents the contribution of thej^{th} cell to the particular ray integral. The factor ($w_{jkl\theta}. f_j$) is equal to the fractional area of the j^{th} image cell intercepted by the ray-sum with index $kl\theta$ as shown in figure (2) [9].

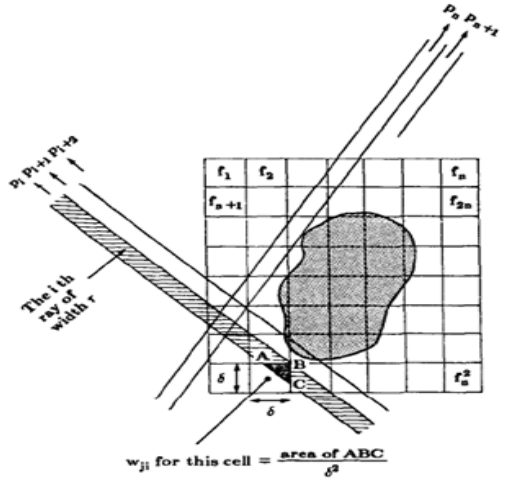

Figure 2: In algebraic methods a square grid is superimposed over the unknown image.

Most of $w_{jkl}. f_j$'s are zero since only a small number of cells contribute to any given ray-sum. This fact will be used to make algorithms faster, where each ray is of width τ. In most cases the ray width is approximately equal to the image cell width [10]. A line integral will now be called a ray-sum image reconstruction of 3D can be obtained by accumulated set from 2D slice, each slice have number of cells and can solving a system of linear equations. In the figure (2), have superimposed a square grid on the image f(x, y) (2D slice in (x,y)), will assume that in each cell the function (x, y) is constant. Letf_j denote this constant value in the j^{th} cell, and let N be the total number of cells. For algebraic techniques a ray is defined somewhat differently. A ray is now a line running through the (x, y)-plane, to illustrate this, have shaded the i^{th} ray in figure (2), If N and the number of ray-sums were small, it would be possible to use conventional matrix theory methods, to invert the system of equations

in eq. (1). In practice N may be a large number and in most cases the number of ray-sums (called later as M) will also have the same magnitude. for these values of M and N the size of the matrix $[w_{jl}]$ in eq. (1) is $M * N$ which precludes any possibility of direct matrix inversion [8]. When M and N have large values there exists iterative method for solving eq. (1), based on the "method of projections" proposed by Kaczmarz [10], and later elucidated further by Tanabe [11]. To explain computational steps involved in these methods, first write eq.(1) in an expanded form [8]:

$$\begin{aligned} &w_{11}f_1 + w_{12}f_2 + w_{13}f_3 + \cdots + w_{1N}f_N = p_1 \\ &w_{21}f_1 + w_{22}f_2 + w_{23}f_3 + \cdots + w_{2N}f_N = p_2 \ldots (2) \\ &w_{M1}f_1 + w_{M2}f_2 + w_{M3}f_3 + \cdots + w_{MN}f_N = p_M \end{aligned}$$

An image represented by $(f_1, f_2, \ldots\ldots\ldots f_N)$, may be considered to be a single point in an N dimensional space. The main idea of the ART algorithm (which is also known as the Kaczmarz method) is to make the estimated image satisfy one equation at a time as illustrated in figure (3)

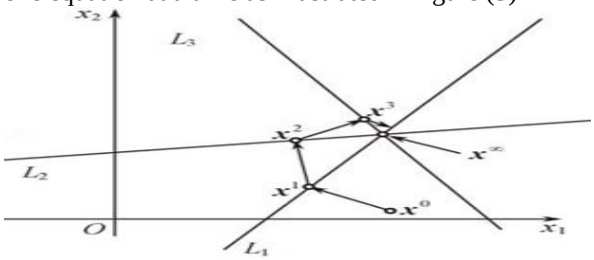

Figure 3: The ART algorithm tries to satisfy each equation at each update.

In each space of the above equations (2) represents a hyperplane. When a unique solution to these equations exists, the intersection of all these hyperplanes is a single point giving that solution. In this example the image only consists of 2 pixels. Where 3 lines: $L1$, $L2$, and $L3$ - represent 3 equations, and their intersection is the solution [5].

For the computer implementation of this method, initial guess of the solution is made. This guess, denoted by $f_1^{(0)}, f_2^{(0)}, \ldots\ldots, f_N^{(0)}$ in the N-dimensional space. In most cases, and In this work, it has been assigned a value of zero to all the initial f_i's. This initial guess is projected on the hyperplane represented by the first equation in (2) giving $\overrightarrow{f^{(1)}}$. $\overrightarrow{f^{(1)}}$ is projected on the hyperplane represented, by the i^{th} equation to yield $\overrightarrow{f^{(2)}}$ and so on. When $\overrightarrow{f^{(i-1)}}$ is projected on the hyperplane represented, by the i^{th} equation to yield $\overrightarrow{f^{(i)}}$ the process can be mathematically described by

$$\overrightarrow{f^{(i)}} = \overrightarrow{f^{(i-1)}} - \frac{\overrightarrow{(f^{(i-1)}} \cdot \overrightarrow{w_i} - p_i)}{\overrightarrow{w_i} \cdot \overrightarrow{w_i}} \overrightarrow{w_i} \quad \ldots (3)$$

Where $\overrightarrow{w^i} = (w_{i1}, w_{i2}, \ldots\ldots, w_{iN})$ and $\overrightarrow{wi}$. $\overrightarrow{wi}$ is the dot product of $\overrightarrow{wi}$ with itself. In applications requiring a large number of views and where large-sized reconstructions are made, the difficulty with using eq. (2) can be in the calculation, storage, and fast retrieval of the weight coefficient [10]. To get around the implementation difficulties, caused by the weight coefficient, several algebraic approaches have been suggested, many of which are approximations to eq.(3). To discuss some of the more implementable approximations, first recast (3) in a slightly different form [8] :

$$f_j^{(i)} = f_j^{(i-1)} + \frac{p_i - q_i}{\sum_{k=1}^{N} w_{ik}^2} w_{ij} \quad \ldots (4)$$

Where

$$q_i = \sum_{k=1}^{N} f_k^{(i-1)} w_{ik} \quad \ldots (5)$$

These equations say that when project the $(i-1)^{th}$ solution onto the i^{th} hyperplane [i^{th} equation in (2)] the gray level of the j^{th} element, whose current value is $f_j^{(i-1)}$ is obtained by correcting its current value by, $\Delta f_j^{(i)}$, where [8]

$$\Delta f_j^{(i)} = f_j^{(i)} - f_j^{(i-1)} = \frac{p_i - q_i}{\sum_{k=1}^{N} w_{ik}} w_{ij} \quad \ldots (6)$$

Note that while ρ_i is the measured ray-sum along the i^{th} ray, q_i may be considered to be the computed ray-sum for the same ray based on the$(i-1)^{th}$ solution for the image gray levels.

The correction Δf_j, to the j^{th} cell is obtained by first calculating the difference between the measured ray-sum and the computed ray-sum, normalizing this difference by $\sum_{k=1}^{N} w_{ik}^2$, and then assigning this value to all the image cells in the i^{th} ray, each assignment being weighted by the corresponding w_{ij}. Most of the w_{jkl} f_j's are zero since only a small number of cells contribute to any given ray-sum. This fact will be used to make algorithms faster.

Generally, a reconstruction needs tens of or even more than a hundred iterations before the solution converges. Details about ART can be found in [12].

Iterative methods consist necessarily of four major steps [9]:

- assumption of the test field,
- calculation of correction,
- application of correction,
- test for convergence

These algorithms differ in the manner in which corrections are applied and presented in brief below.

4-1 Simple ART

In this method corrections are applied to all the cells through which the i^{th} ray passes, before calculating the correction for the next ray. Hence the number of rays per angle of irradiation is not important [9]. In the iterative approach implemented of ART algorithms appear other problem besides the computational efficiency is incorporated the information that used in reconstruction image that cause a problem in the speed of the storage and the access of the information. The reconstruction speed is important in the reconstruction image therefore to solve the ART problems by use high-quality computer unit in terms of speed, processing and storage [8].

4-2 Simultaneous Iterative Reconstruction Technique (SIRT)

In SIRT, the elements of the field function are modified after all the correction values corresponding to individual rays have been calculated. The algorithm is similar to ART but the correction is applied after through all the equation, so only at the end of each iteration the pixel values are update. The change applied to the pixel values is the average value of all the computed changes for the cell. This obvious is solve the problem that a pixel may be crossed by many rays during one iteration by updating the grid for every ray which originally existed in ART algorithms, this mean that the SIRT does not update the image ray by ray, but update the image once per iteration. The SIRT algorithm has however not gained a wide popularity, because it has a big downside. SIRT appears to require a long time for convergence and thus takes a long time for reconstructing an image. For this reason Simultaneous ART was developed. The expression of the Simultaneous Iterative Reconstruction Technique is described as follows [13] :

$$f^{(k+1)} = f^{k} + \frac{1}{\sum w_{ij}} \sum_j \left(N_{i,j} - N_{c,j}^{(k)}\right) w_j \quad \dots (7)$$

Where the j subscript indicates the different measurements, k iterative number, f intensity of each pixel, W matrix of the sensitivity distribution inside the capacitance sensor, $N_{m,j}$ measured ray-sum, $N_{c,j}$ calculated ray-sum [13].

4-3.Simultaneous ART (SART) algorithm

Anderson and Kak [8] proposed a new algorithm, simultaneous the ART, which integrates ART and SIRT algorithms. Is found to be very efficient and superior in the application and reconstructions of good quality and numerical accuracy in only one iteration. Applying a method of correction is similar to the simple ART but composition is similar to SIRT. The main features of SART reduce errors in the approximation of ray integrals of a smooth image by finite sums. To further reduce the noise resulting from the unavoidable but now presumably considerably smaller inconsistencies with real projection data, the correction terms are simultaneously applied for all the rays in one projection; this is in contrast with the ray-by-ray updates in ART. Now that superior results are obtained if instead of sequentially updating pixels on a ray-by-ray basis simultaneously apply to a pixel the average of the corrections generated by all the rays in a projection. For the first ray in a projection computed as before the corrections to be made at every pixel. Instead of actually applying these corrections, store them in a separate array to be called the correction array (the size of which is the same as that of the image array). Then take up the next ray and add the pixel updates generated by this ray to the correction array. And then the next ray, and so on. After through all the rays in a projection, add the correction array (or some fraction thereof) to the image array. This entire process is repeated with every projection.

$$\overrightarrow{f^{(k+1)}} = \overrightarrow{f^{(k)}} + \overrightarrow{a_i} \frac{\rho_i - \overrightarrow{a_i}\,\overrightarrow{f^{(k)}}}{\overrightarrow{a_i}\,\overrightarrow{a_i}} \quad \dots (8)$$

Where the k iterative number, $\overrightarrow{a_i}$ denotes the ith row vector of the array, ρ_i is the measured ray-sum, f gray level distribution [8].

4-4 Multiplicative ART (MART)

The correction strategies of offered above invites the ART of added (or simply ART). When a multiplicated correction, the ART is invites MART. The initial approximation calculated using Eq. (2). The MART technique [5] involves a multiplicative correction to the voxel intensity based on the ratio of the recorded pixel intensity p_i and the projection of voxel intensities $\vec{p}_i$ from the previous iteration k:

$$\vec{f}_j^{k+1} = \vec{f}_j^{k} * \prod Nc_j \ (1 - \lambda(1 - \frac{p_i}{\vec{p}_i})) \quad \dots (9)$$

$$\vec{f}_j^{k+1} = \vec{f}_j^{k} * \prod Nc_j \ (\frac{p_i}{\vec{p}_i})^{\lambda} \quad \dots (10)$$

Where Nc_j is the total number of rays per cell, λ is a relaxation parameter typically chosen between 0 and 2. Elsinga et al. [14] indicate that this algorithm was preferable to that of additive algebraic reconstruction technique, which was shown to leave ART effects or tracer is the reconstructed field. Each voxel's intensity is corrected to satisfy one projection or pixel at a time, with a single iteration being completed only after every projection has been considered. This method has been proven to converge to the maximum information based entropy solution,

which represents the most probable reconstruction based on the recorded projections [6]

5- Preview About Iterative Algorithm

In an iterative algorithm can be thought of as a "closed loop" system. Each loop, referred to as an iteration, usually consists of a projection operation, a comparison of the projected data with the measured data, and a backprojection operation. The backprojection maps the data discrepancies from the projection space to the image space. The backprojected discrepancies will be used to modify the currently estimated image at each iteration [5].

Generally, a reconstruction needs tens of or even more than a hundred iterations before the solution converges [12]. A simultaneous application of the error correction terms as computed for all rays in a given projection was introduced as the SART. To overcome the disadvantage that negative values appear in the reconstruction, another variant, the Maximum-Likelihood Expectation-Maximization algorithms (ML-EM) and the Multiplicative ART, they converge only at small values of their relaxation parameter MART, can be used instead. Although MART algorithms produce less error at convergence compared to additive ART [15]. Solve the problem of speed in SART them devise a new hardware acceleration scheme, employing readily available texture mapping graphics hardware that allows quality 3D cone-beam reconstructions to be obtained at almost interactive speeds [16]. In the our research used the ML-EM algorithm to update algorithm as derived and can be symbolically expressed as

$$f^{\text{next}} = f^{\text{current}} \frac{\text{Backproject}\left\{\frac{\text{measurement}}{\text{project}(x^{\text{current}})}\right\}}{\text{Backproject}\{1\}} \dots (11)$$

Where {**1**} is a vector with elements of 1's. The size of the vector is that of the projection data vector. In this algorithm, the data discrepancy is calculated as a ratio instead of a difference. The distinguishing feature of this algorithm is its non-negativity. If the initial image x^0 does not contain any negative voxels, the image values will never become negative. The usual ML-EM algorithm is derived and used particularly for the emission data reconstruction. Also have transmission-data ML-EM algorithms, too, but they are not as popular. In ART, the image is updating after each projection ray is considered. One way to speed up the convergence rat of an iterative algorithm is to make more frequent image updates as Ordered-Subset Expectation-Maximization algorithm (OS-EM). In an OS-EM algorithm, the projection views are grouped in different sets (called subsets), the algorithm goes through the subsets in a specified order, and the image is updated after each subset is considered. That cause accelerates ML-EM algorithm about approximately 10 time is possible with very lettel increase in noise [5].

6- Result and disscution

In this paper the results that were obtained after the simulation of ART algorithm in cone beam –multi slice helical geometries of CT with these discussions are presented .The simulation result is implemented using MATLAB (version R2013a) programming language and computer system: core i5, 2.3GHZ CPU for the processing. To justify the theory, the results based on MATLAB will be showed. In this work the 3D head-phantom (test image) used for generating the projections for different slices of the reconstruction image shown in figure (4), image size (128 x128x128) pixel .

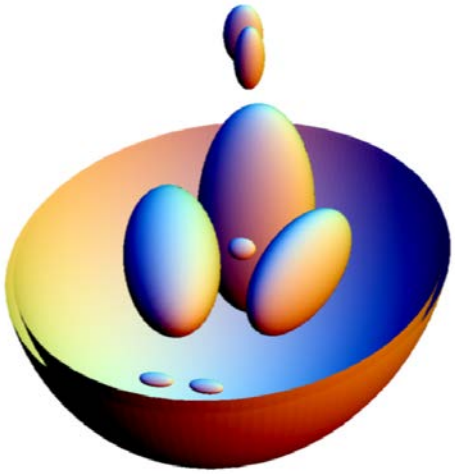

Figure 4: 3D head phantom

Multi-detector CT (MDCT) scanners were used to acquire up to 128 slices, considerably reducing the scanning time compared with single-slice systems and allowing generation of 3D images at substantially lower doses of radiation than single detector fan-beam CT arrays. It provides clear slices images of highly contrasted structures and is extremely useful for evaluating bone. Also MATLAB program was used to obtain a 2D slice from 3D test image to generate a 3D head phantom that can be used to 3D image reconstruction algorithms with Shepp-Logan, this 2D test image that is used widely by researchers in tomography For the simulation result used the modified Shepp-Logan phantom for used with 3D image reconstruction algorithms, the suggested head phantom is the same as the Shepp-Logan except the intensities are changed to yield higher contrast in the image [18]. In cone beam multi slice, has cone angle βis important parameter to obtain projection of 3D object to obtain excellent result must be less than 10° and the anther input

parameter of the X-ray source and detector of object 128 x128 x 128 pixel setting is:
- DSD: distance between source to detector = 1000 mm.
- DSO: distance between x-ray source to iso-center (image center) = 600 mm, DSO parameter must be large enough to ensure that the cone beam is outside of the image at all rotation angles and 360 projections with uniform increment of unity are used.
- The real detector panel pixel density (number of pixels) is parameter with value u=256 mm and v=200 mm. number of detector pixels of x-direction (u) and number of detector pixels of z-direction (axial) (v).

rotation direction (+1 or -1) clockwise or counter-clockwise: when using real data, if you don't know direction, just try +1 or -1, then you can find it in these thesis use direction =1, and interval of angular sampling (degree), if the value is 1, each projection rotates 1 degree. The moving X-ray source and detectors to the next slice to obtain the projections at the next z position to another multi slice. Select cone angel β=10°.

Choosing four slices as shown in the figure (5) and applying ART ,SART and MART to show the best algorithm can be using that gives excellent reconstructed image and fast implementation by multi slice CT in spiral mode cone beam algorithm. Figure (6) shown the sinogram of each projection which selected (1,151,181,201,361) projections, and selected the fifty one, sixty four, sixty seven, seventy five slices and applying algorithms of algebraic reconstruction technique .

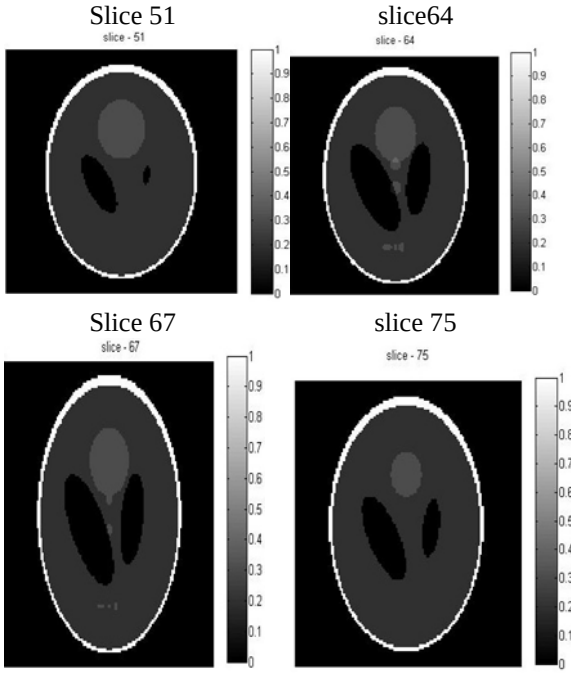

Figure 5: Different slices chosen along the Z-orientation of the original data

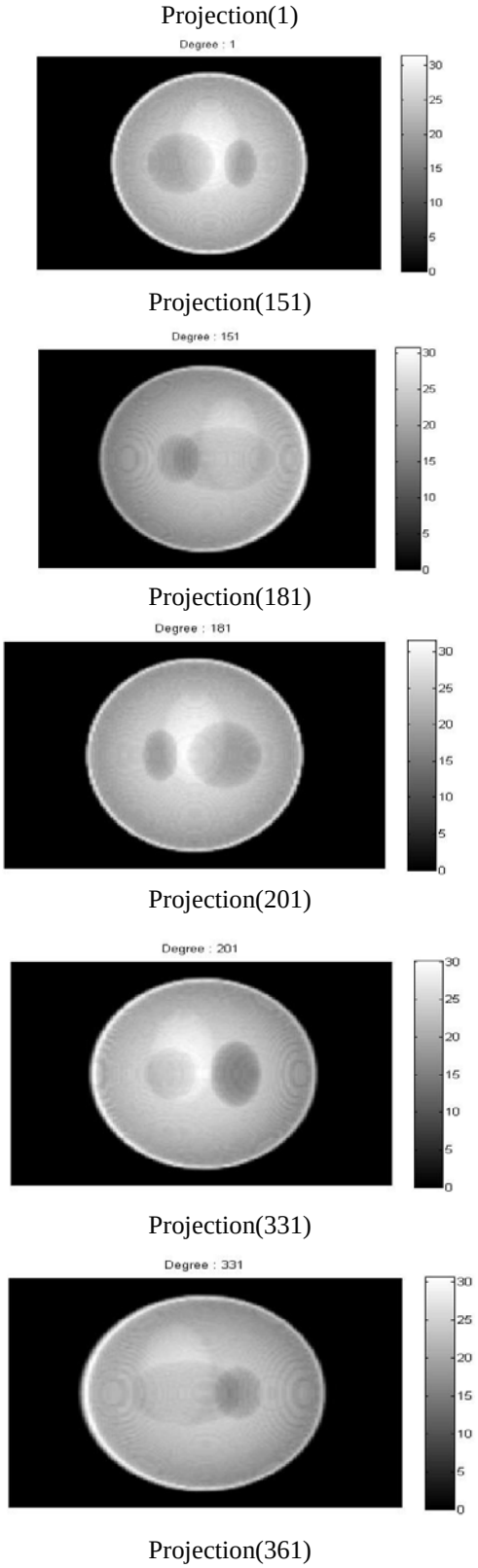

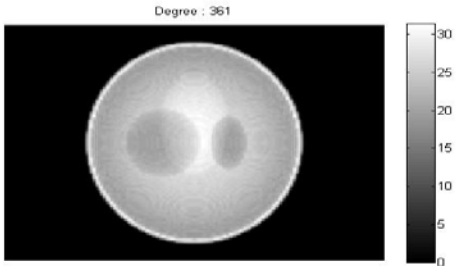

Figure 6: Sinogram of the projection with different cone angle θ =1,151,181,201,331,361 along the orientation.

The computer implementation of the ART and MART algorithms using multi slice CT in spiral geometry, as illustrated in the following steps:

Step 1: it is assumed the cross-sections consist of arrays of unknowns.

Step 2: reconstruction problem can be formulated as a system of linear equations (Radon transform is linear) eq. (2).

Step 3: choosing a finite collection of basis functions and a method to solve the systems are the next steps.

The result of simple ART after 180 iteration as shown in table (1). The best time of performance is obtained of each iteration is 528.96341 sec. to reconstruction volume 128 x 128 x 128 and different conditions of implementation possible the time change in the $\pm$ 4 sec.

Different quality parameters such as root mean square error (RMSE), mean square error (MSE), power signal to noise ratio (PSNR), maximum difference (MD) and normalized absolute error (NAE) used to show the accuracy of reconstructed image with different algorithms.

The mean square error (MSE) is used to qualitatively measure the difference between the original image and the reconstructed image. The MSE is defined as [80]:

$$MSE(\%) = \frac{\hat{f}\,(x,y,z)-f\,(x,y,z)}{\|f(x,y,z)\|^2}\text{x}100\% \quad \dots (12)$$

Let $f\,(x, y,z)$ be an input image and $\hat{f}\,(x, y,z)$ be a reconstructed of $f\,(x,y,z)$ that result from compressing and subsequently decompressing the input.

Signal to noise ratio (PSNR) is used to measure the difference between two images, It is defined by [2]

$$SNR\,ms = \frac{\sum_{x=0}^{M-1}\sum_{y=0}^{N-1}\hat{f}\,(x,y,z)^2}{\sum_{x=0}^{M-1}\sum_{y=0}^{N-1}\left[\hat{f}\,(x,y,z)-f(x,y,z)\right]^2} \quad \dots (13)$$

Where the image are of the size M x N, The root-mean square error, RMSE between *f(x, y,z)* and $\hat{f}(x,y,z)$ is then the squared error averaged over the M x N array, or

$$\text{RMSE} = \left\lfloor \frac{1}{MN}\sum_{x=0}^{M-1}\sum_{y=0}^{N-1}\left[\hat{f}(x,y,z) - f(x,y,z)\right]^2\right\rfloor^{\wedge 1/2} \quad \dots (14)$$

If $\hat{f}(x,y,z)$ is considered to be the reconstructed of the original image *f(x, y,z)* and an error or "noise" signal *e(x, y,z)*.

Normalized absolute error (NAE): it's a numerical difference between the original and reconstructed image.

$$NAE = \frac{\sum_{x=0}^{M-1}\sum_{y=0}^{N-1}|\hat{f}(x,y,z)-f(x,y,z)|}{\sum_{x=0}^{M-1}\sum_{y=0}^{N-1}|f(x,y,z)|} \quad \dots (15)$$

Maximum Distance (MD): error it's the variation of the method of paired Comparisons:

$$MD = max\left(\left|\hat{f}(x,y,z) - f(x,y,z)\right|\right) \quad \dots (16)$$

The quality parameter measurement in ART of slice 64 have the following value of RMSE is 0.2268, PSNR is 54.995, MD is 0.6937, NAE is 3.0746 and MSE is 0.2140

[[[

Table 1: The result of simple ART

slice	RMSE	PSNR	MD	NAE	MSE
Slice51	.2313	54.6687	.6687	3.0676	.2140
Slice64	.2268	54.995	.6937	3.0746	.2058
Slice67	.2255	55.0470	.6917	3.0767	.2034
Slice75	.2262	55.01987	.6724	3.0813	.2047

When applying Eq.(8)The result of SART with ML-EM algorithm is shown in table (2) and obtained number of iteration is reduce to 100 iteration . The best time performance is obtained of each iteration is 507.534263 sec. to reconstruction volume 128 x 128 x 128 of each iteration and different conditions of implementation possible that up to a maximum of $\pm$ 7 sec. The quality parameter measurement in SART of slice 64 have the following value of RMSE is 0.0894, PSNR is 63.0810, MD is -1, NAE is 16.1535 and MSE is 0.0320 ,The SART give best result from ART.

Table 2: The result of SART with 100 iteration

slice	RMSE	PSNR	MD	NAE	MSE
Slice51	0.0904	62.9874	-1	16.1535	0.0327
Slice64	0.0894	63.0810	-1	16.4541	0.0320
Slice67	0.0892	63.1015	-1	16.5234	0.0318
Slice75	0.0895	63.0785	-1	16.4386	0.0320

The result of MART1 in eq.(9) with different value of relaxation parameter as shown in table(3) ,(4)and (5). The best time is obtained of each iteration is 365.38631 sec. to reconstruction volume 128 x 128 x 128 of each iteration and different conditions of implementation possible that up to a maximum of $\pm$ 5sec. with reduce number of iteration to 86. The quality parameter

measurement in MART1 with λ = 0.8 of slice 64 have the following value of RMSE is 0.0020, PSNR is 99, MD is 0.4047, NAE is 0.1283 and MSE is 1.6004 e^{-05} , this excellent result comparing with ART and SART as shown in table (3) .

Table 3: The result of MART1 with λ=.8 and iter=86

slice	RMSE	PSNR	MD	NAE	MSE
Slice51	0.0020	99	0.3944	0.1037	$1.547e^{-05}$
Slice64	0.0020	99	0.4047	0.1283	$1.6004e^{-05}$
Slice67	0.0020	99	0.3765	0.1278	$1.5822e^{-05}$
Slice75	0.0020	99	0.3923	0.1150	$1.5636e^{-05}$

The quality parameter measurement in MART1 with change relaxation parameter to λ = 0.9 of slice 64 have the following value of RMSE is 0.0019 this is minimum value, PSNR is 99 is higher value , MD is 0.3872, NAE is 0.1203 and MSE is $1.4453e^{-05}$ there are kept minimum value as shown in table (4).

Table 4: The result of MART with λ=.9 and iter =86

slice	RMSE	PSNR	MD	NAE	MSE
Slice51	0.0019	99	0.3851	0.0976	$1.4712e^{-05}$
Slice64	0.0019	99	0.3872	0.1203	$1.4453e^{-05}$
Slice67	0.0019	99	0.3585	0.1197	$1.4280e^{-05}$
Slice75	0.0019	99	0.3820	0.1078	$1.4207e^{-05}$

The quality parameter measurement in MART1 with change relaxation parameter to λ = 1 of slice 64 have the following value of Rmse is 0.0018 this is less value from λ =0.9, PSNR is 99 is higher value , MD is 0.3700, NAE is 0.1136 and MSE is 1.3166 e^{-05} these are kept minimum value from result in λ =0.9 as shown in table (5).

Table 5: The result of MART with λ= 1 and iter = 86

slice	Rmse	PSNR	MD	NAE	MSE
Slice51	0.0018	99	0.3764	0.0925	$1.2960e^{-05}$
Slice64	0.0018	99	0.3700	0.1136	$1.3166e^{-05}$
Slice67	0.0018	99	0.3410	0.1130	$1.2994e^{-05}$
Slice75	0.0018	99	0.3640	0.1020	$1.3017e^{-05}$

The result of MART2 in eq.(10) with different value of relaxation parameter as shown in table (6) ,(7) and (8). The best time is obtained of each iteration is 301.45126 sec. to reconstruction volume 128 x 128 x 128 of each iteration and different conditions of implementation possible that up to a maximum of $\pm$ 5 sec. with reduce number f iteration to 80. The quality parameter measurement in MART2 with change relaxation parameter to λ = 1.2 of slice 64 have the following value of RMSE is 0.0017 this is less value from λ =1, PSNR is 99 is higher value , MD is 0.3390, NAE is 0.1037 and MSE is $1.1236e^{-05}$ this are kept minimum value from result in λ =1.

Table 6: The result of MART2 with λ=1.2 and iter. =80

slice	RMSE	PSNR	MD	NAE	MSE
Slice51	0.0017	99	0.3613	0.0852	$1.1235e^{-05}$
Slice64	0.0017	99	0.3390	0.1037	$1.1236e^{-05}$
Slice67	0.0017	99	0.3115	0.1032	$1.1060e^{-05}$
Slice75	0.0017	99	0.3412	0.0934	$1.1220e^{-05}$

The quality parameter measurement in MART2 with change relaxation parameter to λ = 1.2 and reduce number of iteration to 70 to reduce time reconstruction image and found the result of slice 64 have the following value of RMSE is 0.0018, PSNR is 99 is higher value , MD is 0.2736, NAE is 0.1108 and MSE is $1.2617e^{-05}$ this are kept minimum value from previous result and give advantage as shown in table(7).

Table 7: The result of MART with powe λ=1.2 and iter.=70.

slice	RMSE	PSNR	MD	NAE	MSE
Slice51	0.0018	99	0.2665	0.0904	$1.2473e^{-05}$
Slice64	0.0018	99	0.2736	0.1108	$1.2617e^{-05}$
Slice67	0.0018	99	0.2395	0.1102	$1.2444e^{-05}$
Slice75	0.0018	99	0.2605	0.0995	$1.2308e^{-05}$

The quality parameter measurement in MART2 with change relaxation parameter to λ = 0.8 of slice 64 have the following value of RMSE is 0.002 this is value began to increasing from λ =1, PSNR is 99 is higher value , MD, NAE and MSE is also increasing this are give disadvantage of result in reconstruction image as shown in table (8).

Table 8: The result of MART2 with λ=0.8 and iter.=80

slice	Rmse	PSNR	MD	NAE	MSE
Slice51	0.0020	99	0.3928	0.1033	$1.5388e^{-05}$
Slice64	0.0020	99	0.4030	0.1278	$1.5907e^{-05}$
Slice67	0.0020	99	0.3747	0.1273	$1.5733e^{-05}$
Slice75	0.0020	99	0.3908	0.1145	$1.5548e^{-05}$

Table 9: The result of MART2 with λ=2 and iter.=80

slice	Rmse	PSNR	MD	NAE	MSE
Slice51	0.0020	99	0.3944	0.1037	$1.5471e^{-05}$
Slice64	0.0020	99	0.4047	0.1283	$1.6004e^{-05}$
Slice67	0.0020	99	0.3765	0.1278	$1.5828e^{-05}$
Slice75	0.0020	99	0.3923	0.1150	$1.5636e^{-05}$

Table 10: The result of MART2 with λ=2 and iter.=50 .

slice	Rmse	PSNR	MD	NAE	MSE
Slice51	0.0653	99	0	0.62513	$1.7100e^{-05}$
Slice64	0.0618	99	0	0.59635	$1.5300e^{-05}$
Slice67	0.0617	99	0	0.59937	$1.5329e^{-05}$
Slice75	0.0645	99	0	0.62364	$1.6643e^{-05}$

7- Conclusion

The method that implemented can be used for image reconstruction in CT is cone beam multi slice spiral geometry. In this work The main conclusion that can be deduced from the results

obtained from ART algorithm implemented of the cone beam multi slice spiral reconstruction method that ART with different methods (ART, SART, MART1and MART2) applying by using cone beam multi slice spiral geometry in three dimension head phantom image size (128 x 128 x 128) and get the elapsed time and other quality measurement by root mean square error, signal to noise ratio, maximum difference, normalized absolute error and mean square error recorded for each image reconstructed led to ability to compare the quality and performance for the tomographic reconstructed image. The MART1 eq. (9) appeared to give an best output result when comparing result with ART and SART and the best performance efficiency when relaxation parameter λ=1 from λ = 0.9 and λ =0.8 and MART2 (10) appeared to give an best output result and the best performance efficiency when relaxation parameter λ=1.2 from λ=1, λ=0.9 and λ=2 give high performance for reconstructed image and excellent quality objectively this mean the MART2 best than MART1 algorithm with λ=1.2 and number of iteration reduce to 80 iteration. Also have increasing relaxation parameter to 2 to reduce number of iteration and obtained quality of image reconstruction but root mean square error increased.

Reference

[1] A. F. Kopp1, K. Klingenbeck-Regn2, M. Heuschmid1, A. Küttner1, B. Ohnesorge2, T. Flohr2, S. Schaller2, C. D. Claussen1 **"Multislice Computed Tomography:Basic Principles and Clinical Applications''** electromedica 68 (2000) no. 2, German

[2] R. Gonzalez and Richard E. Wood, **"Digital Image Processing**" Third Edition, Pearson international education, 2008.

[3] Henrik Turbell, **"Cone-Beam Reconstruction Using Filtered Backprojection''**, Link¨oping Studies in Science and Technology Dissertation No. 672, February 2001.

[4] Hui Hu, **"Multi-slice helical CT: Scan and reconstruction''**, Med. Phys. 26 .1., January 1999.

[5] Gengsheng Lawrence Zeng, **"Medical Image Reconstruction'',** Springer,New York,2010.

[6] C. H. Atkinson and J. Soria, **"Algebraic Reconstruction Techniques for Tomographic Particle Image Velocimetry''**, 16th Australasian Fluid Mechanics Conference, Australia,2-7 December 2007.

[7] Nargol Rezvani , **"Reconstruction Algorithms in Computerized Tomography''**, London ,CAIM,2009,

[8] KAK. A.C. and M. Slaney, **"Principle of computerized tomographic imaging", New York, 1999.**

[9] **Wojciech Chlewicki, "3D Simultaneous Algebraic Reconstruction Technique for Cone-Beam Projections''**, Patras 2001

[10] S. Kaczmarz. "**Angenaherte anosung von systemen linear gleichungen".** Bull. Acad. Pol. Sci. Lett., 6-8A:355{357, 1937

[11] K. Tanabe. **"Projection method for solving a singular system"**. Numer. Math., 17:203{214, 1971.

[12] Junjun Deng, **"Parallel computing techniques for computed Tomography''**, thesis, University of Iowa,2011.

[13] A. C. Kak and M. Slaney., **"Principles of Computerized Tomography"**, IEEE, 1987.

[14] Elsinga, G. E., Scarano F., Wieneke B. and van Oudheusden B. W., **"Tomographic particle image velocimetry",** California, USA, September, Experiments in Fluids, 41, 2006, 933–947.

[15] Stelios Angeli and Efstathios Stiliaris, **" An Accelerated Algebraic Reconstruction Technique based on the Newton-Raphson Scheme''**, 2009. IEEE

[16] Klaus Mueller.and Roni Yagel Rapid , **"3D Cone-Beam Reconstruction with the Algebraic Reconstruction Technique (ART) by Utilizing Texture Mapping Graphics Hardware''** , at the IEEE Medical Imaging Conference,1998.

[17] Elsinga, G. E., Scarano, F., Wieneke, B. and van Oudheusden, B. W., "**Tomographic particle image velocimetry"**, Experiments in Fluids, 41, 2006.

[18] Noor H. Al-anbari and Dr. Mohammed H. Ali Al-Hayani , **"Design and Construction Three-Dimensional Head Phantom Test Image for the Algorithms of 3D Image Reconstruction''**, CIS Journal ,Vol. 6 No. 1, January 2015

[19] William C. Scarfe, BDS, FRACDS, MSa,*, Allan G. Farman, BDS, PhD, DSc, **"What is Cone-Beam CT and How Does it Wor (2008) 707–730k?''**, 2008 Elsevier, Dent Clin N Am 52 (2008) 707–730